PHYSICAL REVIEW A VOLUME 25, NUMBER 2 FEBRUARY 1982

Muonic Lyman x-ray intensities in pure elements

C. J. Orth, M. E. Schillaci, J. D. Knight, and L. F. Mausner*
Los Alamos National Laboratory, Los Alamos, New Mexico 87545

R. A. Naumann and G. Schmidt†
Princeton University, Princeton, New Jersey 08540

H. Daniel
Los Alamos National Laboratory, Los Alamos, New Mexico 87545
and Technical University of Munich, D-8046 Garching, Germany
(Received 13 August 1981)

Muonic x-ray intensity ratios $[I(Ki)/I(K\alpha)]$ have been measured for 21 pure elements in the range $4 \leq Z \leq 48$. The cyclic variation of these ratios with Z is clearly seen to follow the pattern of the periodic table of the elements over this range. The product of $I(K\beta)/I(K\alpha)$ and nearest-neighbor distance in the pure-element lattices varies approximately linearly with Z within each period.

I. INTRODUCTION

The intensity patterns of the x rays produced in the deexcitation of mesic (K^-,π^-,μ^-) atoms of the pure elements exhibit striking variations with atomic number (Z), variations that appear to correlate with position in the periodic table of the elements. Wiegand and Godfrey[1,2] reported that kaonic x-ray yields reach maximum values near atomic closed-shell elements (i.e., the rare gases) and minimum values roughly midway in Z between these elements. Kunselman[3] and, more recently, Pearce *et al.*[4] observed similar yield variations for pionic x rays. Since both kaons and pions are strongly interacting particles, they are most strongly absorbed by the nucleus from atomic states of low angular momentum l. The observed yield variations are interpreted[1,2] as reflecting the l distribution of mesons in states of high principal quantum number n following Coulomb capture into the atoms. Muons, on the other hand, being weakly interacting particles, exhibit an essentially complete x-ray spectrum from transitions to low-n states; except for H and He, only a few percent are "lost" from the Lyman series by competing Auger transitions. Thus, the muonic Lyman transitions ($K\alpha$, $K\beta$, etc.) provide a convenient monitor for muon capture.

Early muonic x-ray measurements by Quitmann *et al.*[5] indicated that the relative intensity of the higher Lyman lines [e.g., $I(K\beta)/I(K\alpha)$] was smaller for elements near the atomic closed shells than for those midway between. A somewhat similar periodicity was first noted by Zinov *et al.*[6] in the Z/O muon capture ratios in the oxides of metals; they observed that the metallic elements near the middles of the periods captured a proportionately larger share of the muons stopped in the oxides. Although these measurements were made with low-resolution γ-ray detectors, the qualitative features of the results were subsequently confirmed by Knight *et al.*[7] and by Daniel *et al.*[8] using high-resolution systems. Still another periodicity of this kind was observed in an altogether different area by MacKenzie *et al.*,[9] who noted that positron mean annihilation lifetimes in annealed metals exhibit a systematic variation with Z which is similar to that observed for the kaonic and pionic x-ray yields.

Kunselman *et al.*[10] were the first to point out the correlations among these phenomena. They explained the mesic atom results in terms of the meson angular momentum distributions at Coulomb capture: enhanced capture into high-n, low-l states results in diminished x-ray yields for pions and kaons due to nuclear capture before completion of the cascade, just as these same distributions at capture result in increased intensities for the high Lyman transitions of the muons, which do not undergo nuclear absorption during the cascade. They also suggested that since positron annihilation takes place mostly on loosely bound electrons, the

periodic variations of the mesic atom data are associated with periodic density variations of electrons in the outer part of the atom; model calculations[11] were cited in support of this view. The importance of loosely bound electrons in the Coulomb capture process was emphasized also by Schneuwly *et al.*[12]

The variations in muonic x-ray intensity patterns have been examined with considerably improved accuracy and detail in two recent papers by the Munich group. In the first, Bergmann *et al.*[13] reported on measurements of muonic $K\beta/K\alpha$ intensity ratios for 28 pure elements in the range $4 \leq Z \leq 79$, and extracted statistical correlation coefficients between the experimental $K\beta/K\alpha$ intensity ratio and atomic number, atomic radius, atomic volume, and positron lifetime. In the second, von Egidy *et al.*[14] measured the muonic x-ray spectra of 57 oxides ranging from $Z=11$ to $Z=92$ and studied the intensity patterns of both the oxygen and the oxidized element as well as the element/oxygen capture ratio. Their work was directed, in particular, toward identifying the chemical structure factors responsible for the periodic variations observed, and although no analytically simple relationships were established, they concluded that the Coulomb capture process for muons was dominated by the structure or density of the outer electrons of the elements.

In this work, we report on measurements of muonic Lyman x-ray intensity patterns for a series of pure elements between $Z=4$ and $Z=48$, with particular emphasis on the sequence $Z=18-34$. Our choice of targets was influenced by availability of the elements in pure form; enough were chosen to illustrate in detail the Zdependence of several Lyman intensities (up to $7p \rightarrow 1s$, in most cases).

In Sec. II we describe the experimental details and some aspects of the data analysis. In Sec. III we present the data and discuss the results in terms of muon angular momentum distributions at capture.

II. EXPERIMENTAL PROCEDURES

The measurements were made at the Stopped Muon Channel of the Los Alamos Meson Physics Facility (LAMPF). The accelerator was operated at a 5–7% duty factor during these runs, and the channel was tuned to deliver 133 MeV/c negative muons from backward decays of 180 MeV/c pions. The emergent beam contained about 1% electrons and no detectable pions. Most of the measurements were made at time-averaged muon stop rates of $(4-7)\times 10^4$ s^{-1} for typically ~ 3 g/cm^2 of target material measured along the beam axis; higher stop rates resulted in loss of peak resolution in the Ge detector spectra. The beam was collimated by passing through 2.5- to 4.3-cm diam holes in 10-cm-thick lead shielding. Muon stops were detected by a conventional four-element $(123\bar{4})$ plastic scintillator telescope. Details of the telescope-target assembly are given in Ref. 7.

The target materials were of the highest purity practically available, in all cases $>99\%$. Most of the targets consisted of self-supporting metal plates. The Se target consisted of small spheres ($\sim$3-mm diameter) contained in a thin-window Be target frame. The Mn target consisted of a mosaic of small pieces taped to a thin Mylar sheet attached to a Lucite frame. The Sr target was made up of a row of 2-cm-diam cylinders.

The muonic x rays were detected in most cases with an ORTEC coaxial Ge(Li) detector with 10% nominal efficiency. In typical use during accelerator operation the spectrometer system had a resolution of about 2.6 keV at 1.33 MeV. The pulse-height spectra were recorded with a 4096-channel analyzer employing a 100-MHz ADC. Overall coincidence efficiency of the scintillator telescope–x-ray detector combination was determined by comparing singles and coincidence counts and by comparing ratios of prompt and delayed coincidence counts. The prompt time gate was centered on the muon telescope stop signals and the open period was set at 50 ns; the delayed gates spanned another 50-ns time period extending from the late boundary of the prompt period. The delayed spectrum generally included the very low-energy events that were lost from the prompt spectrum because of their slower pulse rise time.

Peak intensities in the muonic x-ray spectra were extracted, wherever possible, with a version of the SAMPO code.[15] In some cases, as when the relevant portions of the spectra were too complex or irregular for the code, peak areas were determined by "hand" integration. Target self-absorption and extended-source corrections were calculated usually with a Los Alamos computer code which had been tested with NBS-calibrated sources both on- and off-axis and with various target thicknesses. The errors shown in the data tables are contributed chiefly by the uncertainties in the measurements of the peak areas. A second significant source of error for x-ray energies below

$\sim$200 keV is the uncertainty in coincidence counting efficiency. Smaller errors occurring at all energies stem from determination of the detector efficiency function, from evaluation of absorption and extended source corrections, and from the more subtle problem of evaluating weak nuclear γ-ray contributions to the x-ray spectrum. The γ-ray contributions were evaluated by comparison of the prompt and delayed spectra, the latter consisting mainly of the γ-ray and low-energy x-ray peaks.

III. RESULTS AND DISCUSSION

The muonic Lyman x-ray intensities measured in this work are given in Table I, where the intensities of the series members are expressed in terms of the ratios to the $2p \rightarrow 1s(K\alpha)$ member. In Table II we compare our $K\beta/K\alpha$ intensity ratio results with other recent data. We note that the agreement between these data is generally within the quoted errors, and thus we combine the data for the purposes of our considerations.

The nature of the overall variations in the quantities is illustrated in Fig. 1(a) and Fig. 2, where we plot the intensity ratios $K\beta/K\alpha$ and $K \geq \theta/K\alpha$, respectively, versus Z up to $Z=50$; all recently reported data are shown. For the $K\beta/K\alpha$ intensity ratio the trend is clear in the upper two-thirds of the Z range: minima occurring near the atomic closed shells and maxima near the half-filled shells. The variation at lower Z is less clear; the lack of data for O, F, and Ne, together with an apparent rapid rise in the ratios with decreasing Z, obscure any other systematic variations. The intensity ratio for the highest Lyman lines, $K \geq \theta/K\alpha$, exhibits (Fig. 2) a sharp Z dependence in the regions where it has been determined. As with the lower ratios it peaks near $Z=25$, indicating a significant population of low-l muon orbits near mid-shell and greatly reduced low-l populations at the closed shells. This indication is supported by the results of a detailed study of the muonic x-ray spectrum of metallic iron by Hartmann *et al.*[21] Trial cascade calculations using a nearly flat initial l distribution, rather than the usual statistical $(2l+1)$ form, best fit their data. We have carried out similar cascade calculations and they too indicate relatively flat l distributions for elements in the middle of the fourth and fifth periods.

Vogel[22] has performed extensive cascade calculations for the third row elements, determining l dis-

TABLE I. Muonic Lyman intensity ratios for pure elements.[a]

Element	Z	$np \rightarrow 1s/2p \rightarrow 1s$ (percent) $n=3$	$n=4$	$n=5$	$n=6$	$n=7$	$n \geq 8$
Be	4	23.5 ±1.6	5.3 ±0.5				
C(graph.)	6	29.0 ±2.0	13.8 ±1.3	4.8 ±1.0			
N(liq.)	7	20.2±0.5	10.9 ±0.5	3.8 ±0.3			
Na	11	11.2 ±0.3	8.0 ±0.3	5.6 ±0.3	2.0 ±0.3	0.30±0.15	
Al	13	10.08±0.36	6.24±0.27	5.27±0.38	3.3 ±0.3	1.7 ±0.7	1.0±0.7
Ar(liq.)	18	7.37±0.15	2.64±0.11	2.26±0.09	2.06±0.08	1.11±0.07	1.4±0.3
K	19	7.6 ±0.3	2.7 ±0.2	2.3 ±0.2	2.1 ±0.2	1.5 ±0.2	2.7±0.2
Ca	20	7.8 ±0.3	2.5 ±0.2	2.5 ±0.2	2.5 ±0.2	1.8 ±0.2	3.7±0.3
Ti	22	9.95±0.30	3.09±0.30	2.5 ±0.2	2.7 ±0.4	1.8 ±0.5	13.0±0.6
Cr	24	11.4 ±0.4	3.4 ±0.4	3.2 ±0.4	2.9 ±0.4	2.2 ±0.4	16.7±1.2
Mn	25	11.3 ±0.4	3.3 ±0.4	2.7 ±0.3	3.8 ±0.4	2.9 ±0.5	16.9±1.3
Co	27	10.2 ±0.4	3.1 ±0.3	2.7 ±0.3	3.9 ±0.6	3.1 ±0.4	13.5±0.5
Cu	29	9.33±0.43	2.6 ±0.1	1.8 ±0.4	1.6 ±0.1	1.6 ±0.1	10.8±0.4
Zn	30	7.69±0.37	2.29±0.21	1.39±0.20	1.21±0.21	0.94±0.22	8.1±1.2
Se(met.)	34	6.5 ±0.4	1.4 ±0.2	1.0 ±0.3	0.7 ±0.2	0.7 ±0.2	4.9±0.5
Sr	38	5.7 ±0.4	1.4 ±0.2				4.5±0.3
Zr	40	7.0 ±0.5	2.7 ±0.6				
Mo	42	8.5 ±0.6	2.6 ±0.5				5.3±0.5
Rh	45	6.8 ±0.6					6.7±0.7
Ag	47	6.71±0.60	1.26±0.30				3.8±1.1
Cd	48	6.1 ±0.6	1.2 ±0.3				1.3±0.3

[a]Errors shown are 1σ.

TABLE II. A comparison of $I(K\beta)/I(K\alpha)$ measurements for some elements.

Element	Z	$I(K\beta)/I(K\alpha)$ (percent) This work	Other work	(Ref. no.)
Be	4	23.5 ±1.6	26.4 ±1.6	13
			28.9 ±0.9	18
C(graph.)	6	29.0 ±2.0	29.65±0.49	13
Na	11	11.2 ±0.3	10.76±0.30	17
Al	13	10.08±0.36	9.33±0.37	13
Ar(liq.)	18	7.37±0.15	7.3 ±0.4	19
Ca	20	7.8 ±0.3	8.00±0.12	13
			7.9 ±0.3	19
Ti	22	9.95±0.30	9.88±0.15	13
			10.2 ±0.3	20
Mn	25	11.3 ±0.4	11.41±0.20	13
			12.1 ±0.9	20
Cu	29	9.33±0.43	10.14±0.40	13
Zn	30	7.69±0.37	7.93±0.30	13
Se(met.)	34	6.5 ±0.4	6.99±0.21	13
			6.74±0.43	16
Mo	42	8.5 ±0.6	8.13±0.42	13
Rh	45	6.8 ±0.6	6.94±0.37	13
Cd	48	6.1 ±0.6	5.86±0.42	13

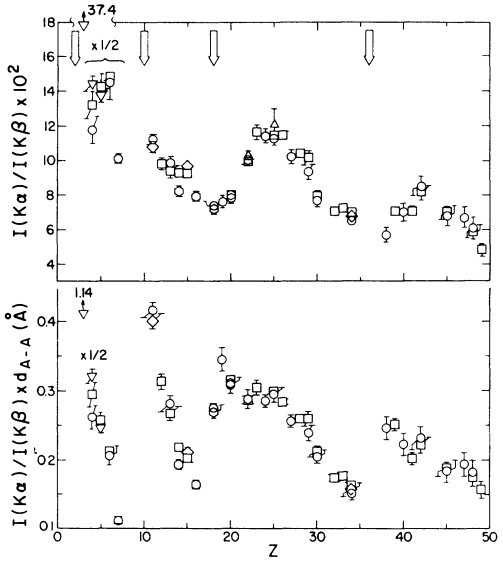

FIG. 1. (a) Muonic Lyman $K\beta/K\alpha$ intensity ratio as a function of atomic number for pure elements. ○ this work, □ Ref. 13, ◇ Ref. 16 and 17, ▽ Ref. 18, ⟨⟩ Ref. 19, △ Ref. 20. The arrows indicate closed atomic shells (rare-gas elements). (b) The product of $I(K\beta)/I(K\alpha)$ and bond length, in Å, as a function of atomic number for pure elements. The symbols are the same as given in (a).

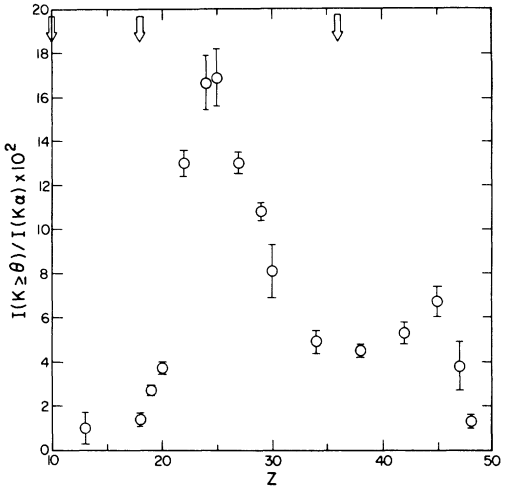

FIG. 2. Muonic Lyman $K \geq \theta/K\alpha$ intensity ratio as a function of atomic number for pure elements measured only in this work. The arrows indicate closed atomic shells (rare-gas elements).

tributions at $n = 17$. Fits were made with the function $P(l) \sim a + bl + cl^2$, and all three coefficients were determined to be positive in each case. Thus, in contrast to the elements in the middle of the fourth and fifth periods, calculations indicate that the third-period elements have l distributions that rise more steeply than statistical. We note the lack of any well-defined peak in the third-period data.

It is instructive to examine the relationship of the measured spectral variations to atomic size. Condo[23] pointed out that kaonic x-ray intensities correlate strongly with atomic diameter in pure element targets. Also, in studies by our group of the muonic x-ray spectra of carbon in diamond and graphite and in various nonhydrogeneous compounds, evidence has been found that the carbon $K\beta/K\alpha$ intensity ratio varies inversely with carbon-atom—to—nearest-neighbor distance.[24] We present the data under consideration here in a form that explicity includes this distance parameter; in Fig. 1(b), we plot the quantity $K\beta/K\alpha \times d_{A-A}$ versus Z, taking our nearest-neighbor distances, d_{A-A}, from a handbook tabulation[25] without regard to crystal structure type. One sees that $K\beta/K\alpha \times d_{A-A}$ varies approximately linearly with Z in each period. Given that $K\beta/K\alpha$ (or any other intensity ratio) is a function of complicated electronic structure factors whose interplay is only crudely relected in the measured quantities we have at our disposal, it is noteworthy that the data as plotted in Figs. 1(a) and 1(b) are as smooth as they

are. We note that a similar plot using $K \geq \theta / K\alpha \times d_{A-A}$ does not yield a linear relationship.

The display of the data in Figs. 1(a) and 1(b) illustrates two problems that remain to be solved: the acquisition of data for the missing elements such as Sc, Ga, and Rb, and the evaluation of "best" values for the elements that have been measured. The statement is sometimes made that relative to our ability to calculate muonic x-ray intensity ratios on a realistic basis, data disagreements or uncertainties of the order of 10% or even 20% are not significant. We believe that this point of view overlooks an important feature of the development of a theory of meson capture. The ability to measure and to recognize small discontinuities in presumed trends with some level of confidence (e.g., between $Z=22$ and $Z=30$) could allow the identification of structure factors and correlations that might otherwise be neglected in the modeling process.

ACKNOWLEDGMENTS

We express our gratitude to the LAMPF technical staff and operating crew for their assistance and cooperation in providing the irradiations, and to Dr. J. E. Sattizahn for his support and encouragement during the course of this work. Three of us (R. A. N., G. S., and H. D.) thank Dr. L. Rosen and his staff for the kind hospitality we have received during our stays at Los Alamos. This work was supported by the U. S. Department of Energy.

---

*Present address: Brookhaven National Laboratory, Upton, New York 11973.

†Present address: Swiss Institute for Nuclear Research, CH-5234, Villigen.

[1]C. E. Wiegand and G. L. Godfrey, Phys. Rev. A 9, 2282 (1974).

[2]G. L. Godfrey and C. E. Wiegand, Phys. Lett. B 56, 255 (1975).

[3]R. Kunselman, Lawrence Berkeley Laboratory Report No. UCLRL-18654 (unpublished).

[4]R. M. Pearce, G. A. Beer, M. S. Dixit, S. K. Kim, J. A. Macdonald, G. R. Mason, A. Olin, C. Sabev, W. C. Sperry, and C. Wiegand, Can. J. Phys. 57, 2084 (1979).

[5]D. Quitmann, R. Engfer, U. Hegel, P. Brix, G. Backenstoss, K. Goebel, and B. Stadler, Nucl. Phys. 51, 609 (1964).

[6]V. G. Zinov, A. D. Konin, and A. I. Mukhin, Yad. Fiz. 2, 859 (1965) [Sov. J. Nucl. Phys. 2, 613 (1966)].

[7]J. D. Knight, C. J. Orth, M. E. Schillaci, R. A. Naumann, H. Daniel, K. Springer, and H. B. Knowles, Phys. Rev. A 13, 43 (1976).

[8]H. Daniel, W. Denk, F. J. Hartmann, W. Wilhelm, and T. von Egidy, Phys. Rev. Lett. 41, 853 (1978).

[9]I. K. MacKenzie, T. E. Jackman, and N. Thrane, Phys. Rev. Lett. 34, 512 (1975).

[10]R. Kunselman, J. Law, M. Leon, and J. Miller, Phys. Rev. Lett. 36, 446 (1976).

[11]M. Leon and J. H. Miller, Nucl. Phys. A282, 461 (1977).

[12]H. Schneuwly, V. I. Pokrovsky, and L. I. Ponomarev, Nucl. Phys. A312, 419 (1978).

[13]R. Bergmann, H. Daniel, T. von Egidy, F. J. Hartmann, J. J. Reidy, and W. Wilhelm, Z. Phys. A 291, 29 (1979).

[14]T. von Egidy, W. Denk, R. Bergmann, H. Daniel, F. J. Hartmann, J. J. Reidy, and W. Wilhelm, Phys. Rev. A 23, 427 (1981).

[15]J. T. Routti and S. G. Prussin, Nucl. Instrum. and Meth. 72, 125 (1969). Adapted for Los Alamos use by B. R. Erdal.

[16]K. Kaeser, T. Dubler, B. Robert-Tissot, L. A. Schaller, L. Schellenberg, and H. Schneuwly, Helv. Phys. Acta 52, 238 (1979).

[17]K. Kaeser, B. Robert-Tissot, L. A. Schaller, L. Schellenberg, and H. Schneuwly, Helv. Phys. Acta 52, 304 (1979).

[18]C. R. Cox, G. W. Dodson, M. Eckhause, R. D. Hart, J. R. Kane, A. M. Rushton, R. T. Siegel, R. E. Welsh, A. L. Carter, M. S. Dixit, E. P. Hincks, C. K. Hargrove, and H. Mes, Can. J. Phys. 57, 1746 (1979).

[19]L. F. Mausner, R. A. Naumann, J. A. Monard, and S. N. Kaplan, Phys. Rev. A 15, 479 (1977).

[20]D. Kessler, H. L. Anderson, M. S. Dixit, H. J. Evans, R. J. McKee, C. K. Hargrove, R. D. Barton, E. P. Hinks, and J. D. McAndrew, Phys. Rev. Lett. 18, 1179 (1967).

[21]F. J. Hartmann, T. von Egidy, R. Bergmann, M. Kleber, H.-J. Pfeiffer, K. Springer, and H. Daniel, Phys. Rev. Lett. 37, 331 (1976).

[22]P. Vogel, Phys. Rev. A 22, 1600 (1980).

[23]G. T. Condo, Phys. Rev. Lett. 33, 126 (1974).

[24]J. D. Knight, unpublished data.

[25]*Handbook of Chemistry and Physics, 61st ed.*, edited by R. C. Weast (CRC Press, Cleveland, Ohio, 1980–1981).